Finite-Time Nonsingular Terminal Sliding Mode Control for 3D Trajectory Tracking of a Quadrotor UAV under Exogenous Disturbances

Edin Avdukic, Almir Salihbegovic, Emir Sokic and Nedim Osmic[1]

Abstract— **This paper presents a nonsingular terminal sliding mode control (NTSMC) strategy for robust three-dimensional (3D) trajectory tracking of a quadrotor unmanned aerial vehicle (UAV) operating in the presence of external disturbances and modeling uncertainties. The proposed controller is designed using the full nonlinear dynamics of the quadrotor and ensures finite-time convergence of the sliding variables and tracking errors without introducing singularities in the control law. A Lyapunov-based stability analysis is provided to demonstrate finite-time stability of the closed-loop system. The effectiveness of the proposed approach is evaluated through comparative simulations against representative state-of-the-art sliding mode control strategies. Numerical simulations are conducted under multiple operating scenarios, including large initial deviations and persistent external perturbations. The results demonstrate that the proposed NTSMC scheme achieves improved tracking accuracy, enhanced robustness, and a more favorable transient response compared to the considered benchmark controllers.**

I. Introduction

Quadrotor unmanned aerial vehicles (UAVs) have attracted considerable research and industrial interest over the last decade due to their maneuverability, compact structure, and vertical take-off and landing capability. These features make them suitable for numerous applications, including aerial inspection, surveillance, environmental monitoring, mapping, and autonomous navigation [1]–[4]. Their ability to operate in structured as well as unstructured environments has established quadrotors as one of the most important aerial robotic platforms. Despite their mechanical simplicity, quadrotor UAVs exhibit highly nonlinear and underactuated dynamics, involving six degrees of freedom (DoF) controlled by only four independent inputs. As a consequence, controller design remains challenging due to strong nonlinear coupling effects, external disturbances, and parameter uncertainties.

Conventional quadrotor control strategies were mainly based on proportional–integral–derivative (PID), linear–quadratic regulator (LQR), and backstepping methods [5], [6]. Although satisfactory performance can be achieved in nominal operating conditions, these approaches often become less effective in disturbance-affected environments. This limitation motivated the development of robust nonlinear control methods suitable for aggressive maneuvers and uncertain operating conditions [1], [7]. Among robust nonlinear techniques, sliding mode control (SMC) has been extensively investigated because of its strong robustness properties with respect to matched disturbances and model uncertainties [8]–[13]. Nevertheless, several shortcomings remain in the existing literature. Many studies rely on simplified or reduced-order models that do not fully capture the coupled nonlinear dynamics of the quadrotor system. Moreover, rigorous finite-time Lyapunov stability proofs for the complete nonlinear model are frequently omitted [8]–[10], [14]–[17]. In addition, assumptions involving ideal initial conditions or implicit removal of the reaching phase may produce overly optimistic conclusions regarding robustness and chattering behavior under practical operating conditions. Although first-order SMC (FOSMC) achieves strong disturbance rejection capabilities, the discontinuous switching action introduces chattering, which may excite unmodeled dynamics and deteriorate actuator performance [2], [7]. To alleviate this issue, higher-order sliding mode approaches have been proposed. In particular, the second-order SMC (SOSMC) strategy reported in [3] achieved finite-time convergence and improved tracking performance using the complete nonlinear quadrotor model while incorporating a high-gain adaptation (HGA) mechanism for chattering attenuation. Further enhancement of robustness and transient response is still desirable, especially in the simultaneous presence of matched and unmatched disturbances. Terminal SMC (TSMC) offers finite-time convergence properties; however, classical formulations may suffer from singularities. Nonsingular terminal SMC (NTSMC) addresses this drawback by employing nonlinear sliding manifolds that preserve finite-time convergence without singular behavior. However, many existing NTSMC-based quadrotor controllers are still formulated using simplified system representations or without explicitly addressing both matched and unmatched disturbances within a unified stability framework. In contrast, the method proposed in this paper is derived from the complete nonlinear 6-DoF quadrotor model and explicitly incorporates both disturbance classes into the controller synthesis and stability analysis, resulting in a more realistic assessment of closed-loop performance.

In this paper, an NTSMC strategy is proposed for robust three-dimensional (3D) trajectory tracking of a quadrotor UAV. The developed controller guarantees finite-time convergence of tracking errors while maintaining robustness against external perturbations and modeling uncertainties. Closed-loop stability is established through Lyapunov analysis.

[1]All authors are with Department for Automatic Control and Electronics, Faculty of Electrical Engineering, University of Sarajevo, 71000 Sarajevo, Bosnia and Herzegovina, {almir.salihbegovic,esokic,nosmic}@etf.unsa.ba

The main contributions of this work are summarized as follows:

- Development of the NTSMC-based control framework for 3D trajectory tracking of a quadrotor UAV, formulated using the complete nonlinear 6-DoF model and explicitly accounting for coupling effects.
- Lyapunov-based finite-time stability analysis that incorporates modeling uncertainties and external disturbances, providing rigorous robustness guarantees.
- Comprehensive comparative evaluation with FOSMC and SOSMC approaches under realistic disturbance scenarios, highlighting improved robustness and transientperformance of the proposed method.
- Analysis of the trade-off between chattering reduction and robustness through the incorporation of a HGA mechanism.

The remainder of the paper is organized as follows. Section II introduces the nonlinear quadrotor model. Section III presents the proposed NTSMC design and provides the corresponding stability analysis. Simulation studies are reported in Section IV, while conclusions are provided in Section V.

II. Kinematic and Dynamic Model of the Quadrotor UAV

The quadrotor UAV is modeled as a rigid-body aerial platform driven by four rotors mounted symmetrically around the vehicle's center of mass at a distance l. Two rotors rotate clockwise, while the remaining two rotate counterclockwise to compensate for reaction torques and maintain yaw equilibrium. Each rotor generates an aerodynamic thrust proportional to the square of its angular velocity. The vehicle has 6-DoF: three translational and three rotational. Two coordinate systems are defined: the inertial frame $\{g\}$, representing a fixed global reference, and the body-fixed frame $\{o\}$, attached to the center of mass of the quadrotor (see Fig. 1). The position in the inertial frame is given by (x, y, z), while orientation is represented using Euler angles roll ϕ, pitch θ, and yaw ψ. Linear velocities (u, v, w) and angular velocities (P, Q, R) are expressed in the body-fixed frame.

A. Forces and Moments

Each rotor produces a thrust

$$F_i = b\Omega_i^2, \quad i = 1, 2, 3, 4, \tag{1}$$

where b is the thrust coefficient and Ω_i is the i-th rotor angular velocity. The total thrust along the body z-axis is

$$T_z = \sum_{i=1}^{4} F_i = b(\Omega_1^2 + \Omega_2^2 + \Omega_3^2 + \Omega_4^2). \tag{2}$$

Gravity in the inertial frame is

$$\mathbf{F}_g^{\{g\}} = \begin{bmatrix} 0 & 0 & -mg \end{bmatrix}^T, \tag{3}$$

and in the body-fixed frame as follows

$$\mathbf{F}_g^{\{o\}} = mg \begin{bmatrix} s_\theta & -s_\phi c_\theta & -c_\phi c_\theta \end{bmatrix}^T, \tag{4}$$

where $s_\alpha = \sin(\alpha)$ and $c_\alpha = \cos(\alpha)$. The control torques generated by differential rotor speeds are

$$\tau = \begin{bmatrix} \tau_x \\ \tau_y \\ \tau_z \end{bmatrix} = \begin{bmatrix} bl(\Omega_1^2 - \Omega_3^2) \\ bl(\Omega_4^2 - \Omega_2^2) \\ d(\Omega_2^2 + \Omega_4^2 - \Omega_1^2 - \Omega_3^2) \end{bmatrix}, \tag{5}$$

with d denoting the drag coefficient due to rotor rotation. The overall control input vector is

$$\mathbf{u}_c = \begin{bmatrix} T_z & \tau_x & \tau_y & \tau_z \end{bmatrix}^T. \tag{6}$$

B. Translational Kinematics and Dynamics

The transformation from body-frame velocities to inertial-frame position derivatives is given by .

$$\dot{x} = c_\theta c_\psi u + (s_\phi s_\theta c_\psi - c_\phi s_\psi)\, v + (c_\phi s_\theta c_\psi + s_\phi s_\psi)\, w, \tag{7}$$

$$\dot{y} = c_\theta s_\psi u + (s_\phi s_\theta s_\psi + c_\phi c_\psi)\, v + (c_\phi s_\theta s_\psi - s_\phi c_\psi)\, w, \tag{8}$$

$$\dot{z} = -s_\theta u + s_\phi c_\theta v + c_\phi c_\theta w. \tag{9}$$

Translational dynamics in the body-fixed frame is given by

$$\dot{u} = Rv - Qw + g s_\theta, \tag{10}$$

$$\dot{v} = Pw - Ru - g s_\phi c_\theta, \tag{11}$$

$$\dot{w} = Qu - Pv - g c_\phi c_\theta + \frac{T_z}{m} + d_T, \tag{12}$$

where $d_T(t)$ is a bounded disturbance in the thrust channel.

C. Rotational Dynamics

Rotational dynamics follow the rigid-body Euler equations:

$$\dot{P} = \frac{I_{yy} - I_{zz}}{I_{xx}} QR + \frac{\tau_x}{I_{xx}} - \frac{I_{zzm}}{I_{xx}} Q W_G + d_{\tau_x}, \tag{13}$$

$$\dot{Q} = \frac{I_{zz} - I_{xx}}{I_{yy}} PR + \frac{\tau_y}{I_{yy}} - \frac{I_{zzm}}{I_{yy}} P W_G + d_{\tau_y}, \tag{14}$$

$$\dot{R} = \frac{I_{xx} - I_{yy}}{I_{zz}} PQ + \frac{\tau_z}{I_{zz}} + d_{\tau_z}, \tag{15}$$

where I_{xx}, I_{yy}, I_{zz} are the principal moments of inertia, I_{zzm} is the rotor moment of inertia about the z-axis, and d_{τ_i} are bounded disturbance torques.

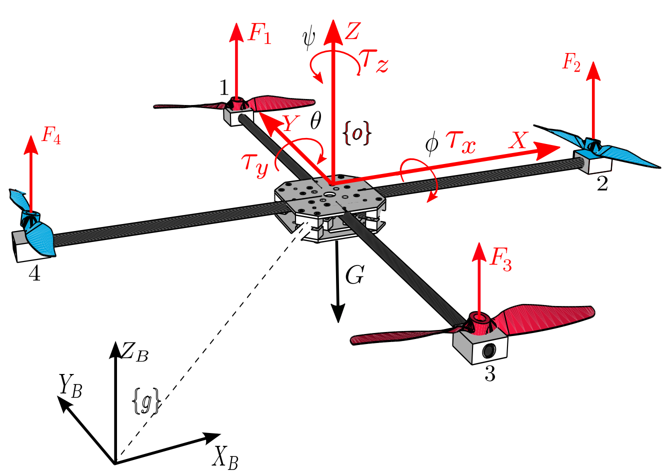

Fig. 1: Quadrotor UAV configuration

D. Euler Angle Kinematics

The relationship between body angular velocities and Euler angle rates is

$$\dot{\phi} = P + Qs_\phi t_\theta + Rc_\phi t_\theta, \tag{16}$$

$$\dot{\theta} = Qc_\phi - Rs_\phi, \tag{17}$$

$$\dot{\psi} = Q\frac{s_\phi}{c_\theta} + R\frac{c_\phi}{c_\theta}. \tag{18}$$

This completes the nonlinear 6-DoF model of the quadrotor UAV, capturing translational-rotational coupling, gravitational effects, and nonlinear coordinate transformations [18]. This formulation provides the basis for the controller design discussed in the following section.

III. NTSMC Design for Robust 3D Trajectory Tracking of a Quadrotor UAV

In this section, the NTSMC technique is adopted in order to achieve finite-time convergence of the tracking errors while avoiding singularities typically associated with classical TSMC formulations. The NTSMC algorithm is designed for the four directly actuated variables of the quadrotor UAV. The control inputs (the total thrust and three control torques) directly affect the altitude z and attitude variables ϕ, θ and ψ, while the horizontal positions x and y are indirectly controlled through the coupling between translational and rotational dynamics.

A. NTSMC-Based Altitude Control Design

The objective of the altitude control subsystem is to ensure accurate tracking of the desired altitude z_{ref} by designing a NTSMC that guarantees finite-time convergence of the altitude tracking error. The tracking error associated with the altitude dynamics is defined as

$$e_z = z - z_{ref}, \tag{19}$$

while the corresponding sliding variable is designed as

$$\sigma_z = e_z + \frac{1}{c_{1z}}\dot{e}_z^{\frac{p}{q}}, \tag{20}$$

where z_{ref} denotes the desired altitude trajectory and $c_{1z} > 0$ is a design parameter. The integers p and q are selected as odd numbers satisfying $1 < \frac{p}{q} < 2$. The adopted nonsingular terminal sliding surface (20) ensures finite-time convergence of the tracking error while avoiding singularities that may arise in classical terminal sliding mode formulations. The equivalent control term is obtained using the sliding condition $\dot{\sigma}_z = 0$, i.e.

$$\dot{\sigma}_z = \dot{e}_z + \frac{1}{c_{1z}}\frac{p}{q}\dot{e}_z^{(\frac{p}{q}-1)}\ddot{e}_z = 0. \tag{21}$$

Differentiating (19) twice and substituting the result into (21) yields

$$\ddot{z} = \ddot{z}_{ref} - c_{1z}\frac{q}{p}\dot{e}_z^{(2-\frac{p}{q})}. \tag{22}$$

From (9), it follows that

$$\ddot{z} = -c_\theta\dot{\theta}u - s_\theta\dot{u} + \dot{A}_1 v + A_1\dot{v} + A_2\dot{w} + \dot{A}_2 w, \tag{23}$$

where the auxiliary variables $A_1 = c_\theta s_\phi$ and $A_2 = c_\theta c_\phi$ are introduced for notational compactness. By substituting the quadrotor dynamics into the sliding condition and equating (22) and (23), while considering (12), the equivalent control term can be expressed as

$$T_{zeq} = \frac{m}{A_2}\Big[\ddot{z}_{ref} - c_{1z}\frac{q}{p}\dot{e}_z^{(2-\frac{p}{q})} + c_\theta\dot{\theta}u + s_\theta\dot{u} - \dot{A}_1 v \\ -A_1\dot{v} - \dot{A}_2 w - A_2 Qu + A_2 Pv + gA_2^2\Big], \tag{24}$$

where $c_{1z} \in \mathbb{R}^+$. To ensure convergence toward the sliding surface, the switching control term

$$T_{zconv} = -c_{2z}\,\mathrm{sgn}(\sigma_z), \tag{25}$$

is introduced, where $c_{2z} > 0$ is a design parameter. The total altitude control is now designed as

$$T_z = T_{zeq} + T_{zconv}. \tag{26}$$

B. NTSMC-Based Attitude Control Design

The attitude control subsystem regulates the quadrotor orientation in order to ensure the desired motion of the vehicle. The objective of the attitude control subsystem is to stabilize the quadrotor rotational dynamics and ensure tracking of the desired Euler angles $(\phi_{ref}, \theta_{ref}, \psi_{ref})$ by generating the control torques τ_x, τ_y and τ_z. The attitude controller is composed of three independent NTSMC loops designed for the roll, pitch and yaw angles.

1) Roll Angle Controller Design: The roll motion corresponds to the rotation around the body x-axis. Therefore, the roll tracking error is defined as

$$e_\phi = \phi - \phi_{ref}. \tag{27}$$

The corresponding nonsingular terminal sliding variable is selected as

$$\sigma_\phi = e_\phi + \frac{1}{c_{1\phi}}\dot{e}_\phi^{\frac{p}{q}}. \tag{28}$$

The equivalent control component is obtained by differentiating the sliding variable and imposing the sliding condition $\dot{\sigma}_\phi = 0$, i.e.

$$\dot{\sigma}_\phi = \dot{e}_\phi + \frac{1}{c_{1\phi}}\frac{p}{q}\dot{e}_\phi^{(\frac{p}{q}-1)}\ddot{e}_\phi = 0, \tag{29}$$

which leads to

$$\ddot{\phi} = \ddot{\phi}_{ref} - c_{1\phi}\frac{q}{p}\dot{e}_\phi^{(2-\frac{p}{q})}. \tag{30}$$

Differentiating the roll dynamics given in (16) leads to

$$\ddot{\phi} = \dot{P} + \dot{Q}A_3 + Q\dot{A}_3 + \dot{R}A_4 + R\dot{A}_4, \tag{31}$$

where the auxiliary quantities $A_3 = s_\phi t_\theta$ and $A_4 = c_\phi t_\theta$ are defined to simplify the notation. Substituting the quadrotor dynamic equations into the sliding condition and setting (30) equal to (31), while also taking (13) into account, the equivalent control component can be written as

$$\tau_{xeq} = I_{XX}\Big[\ddot{\phi}_{ref} - c_{1\phi}\frac{q}{p}\dot{e}_\phi^{(2-\frac{p}{q})} - a_1 QR + \\ + a_2 QW_G - \dot{Q}A_3 - Q\dot{A}_3 - \dot{R}A_4 - \dot{A}_4 R\Big], \tag{32}$$

where $a_1 = \frac{I_{YY}-I_{ZZ}}{I_{XX}}$ and $a_2 = \frac{I_{ZZM}}{I_{XX}}$ are introduced to make the expression more compact. To enforce convergence toward the sliding surface, the switching control component is introduced as

$$\tau_{xconv} = -c_{2\phi}\text{sgn}(\sigma_\phi), \tag{33}$$

where $c_{2\phi} > 0$ is a design parameter. The total roll control torque is therefore given by

$$\tau_x = \tau_{xeq} + \tau_{xconv}. \tag{34}$$

2) Pitch and Yaw Controller Design: The objective of the pitch and yaw control subsystem is to ensure accurate tracking of the desired pitch and yaw angles θ_{ref} and ψ_{ref} by designing NTSMC-based control laws for the corresponding rotational dynamics. The control laws for the pitch and yaw channels are derived analogously to the roll controller by applying the same NTSMC design procedure. The resulting control torques are expressed as

$$\tau_y = \tau_{yeq} - c_{2\theta}\text{sgn}(\sigma_\theta) \tag{35}$$

$$\tau_z = \tau_{zeq} - c_{2\psi}\text{sgn}(\sigma_\psi), \tag{36}$$

with the equivalent control components designed as

$$\begin{aligned}\tau_{yeq} =& \frac{I_{YY}}{c_{1\theta}}\left[\ddot{\theta}_{ref} - c_{1\theta}\frac{q}{p}\dot{e}_\theta^{(2-\frac{p}{q})} - b_1 PRc_\phi + \right.\\ &\left. -b_2 PW_G c_\phi + PQs_\phi + \dot{R}s_\phi + PRc_\phi\right],\end{aligned} \tag{37}$$

$$\begin{aligned}\tau_{zeq} =& \frac{I_{ZZ}}{A_6}\left[\ddot{\psi}_{ref} - c_{1\psi}\frac{q}{p}\dot{e}_\psi^{(2-\frac{p}{q})} - Q\dot{A}_5 + \right.\\ &\left. -\dot{Q}A_5 - R\dot{A}_6 - d_1 A_6 PQ\right],\end{aligned} \tag{38}$$

where $b_1 = \frac{I_{ZZ}-I_{XX}}{I_{YY}}$, $b_2 = \frac{I_{ZZM}}{I_{YY}}$, $d_1 = \frac{I_{XX}-I_{YY}}{I_{ZZ}}$, $A_5 = \frac{s_\phi}{c_\theta}$, $A_6 = \frac{c_\phi}{c_\theta}$, while $c_{1\phi}, c_{2\phi}, c_{1\theta}$ and $c_{2\theta}$ represent positive controller design parameters.

3) Stability Analysis: The stability of the proposed NTSMC control scheme can be established using Lyapunov theory. Consider the Lyapunov candidate function

$$V = \frac{1}{2}\sigma_i^2 \tag{39}$$

where σ_i denotes the sliding variable associated with the corresponding controlled subsystem. The derivative of V is

$$\dot{V} = \sigma_i\dot{\sigma}_i. \tag{40}$$

Substituting the control law into the sliding dynamics yields

$$\dot{\sigma}_i = -c_{2i}\text{sgn}(\sigma_i) + d_i \tag{41}$$

where d_i represents a bounded disturbance. Assuming that

$$|d_i| \leq \Delta_i, \tag{42}$$

the derivative of the Lyapunov function satisfies

$$\dot{V} \leq -(c_{2i} - \Delta_i)|\sigma_i|. \tag{43}$$

Therefore, if the gain is selected such that

$$c_{2i} = \Delta_i + \alpha,\ \alpha > 0, \tag{44}$$

the condition $\dot{V} < -\alpha\sqrt{V}$ is satisfied, which guarantees convergence of the sliding variables to zero in finite time. Consequently, the tracking errors of the attitude subsystem converge to zero in finite time. This ensures that the closed-loop system trajectories reach the sliding surface in finite time and remain on it thereafter.

IV. SIMULATION RESULTS

This section presents simulation results for the quadrotor UAV system under realistic disturbance-affected conditions through three representative scenarios. The objective is to evaluate the performance, robustness, and practical implementation aspects of the proposed control strategy. In particular, the proposed *NTSMC* controller is compared with *FOSMC* [7] and *SOSMC* [3]. The first scenario investigates practical implementation aspects by analyzing chattering reduction using the HGA mechanism [3]. The second scenario provides a comparative evaluation of NTSMC with conventional sliding mode approaches under persistent disturbances, while the third examines robustness during aggressive maneuvers and strong disturbance conditions. All simulations were performed in MATLAB/Simulink using a fixed-step solver with a sampling time of $T_s = 1\,\text{ms}$, corresponding to a control update frequency of $1\,\text{kHz}$. This setting is representative of real-time quadrotor control systems and suitable for digital implementation. The system parameters, together with the FOSMC and SOSMC controller parameters, were adopted from [7] and [3], while the NTSMC parameters were selected as $c_1 = [80,\ 10,\ 10,\ 60]$ and $c_2 = [225,\ 20,\ 20,\ 1]$, with $p = 5$ and $q = 3$ for the $[z,\ \phi,\ \theta,\ \psi]$ channels. The controller gains were tuned using a trial-and-error procedure focused on ensuring robust closed-loop stability under disturbances rather than optimizing transient response. Consequently, the reported results reflect the intrinsic robustness of the proposed control strategy instead of performance achieved through aggressive parameter tuning.

Scenario 1 – Chattering reduction using HGA mechanism

It is well known that discontinuous switching control laws may induce high-frequency chattering in system states and control inputs. While this switching improves robustness in theory, it is undesirable in practice due to increased actuator activity and potential performance degradation. To address this, the HGA strategy is incorporated into the NTSMC framework to attenuate switching intensity while preserving its robustness properties. In this scenario, the Vivian curve is selected as the reference trajectory, with the perturbed initial condition $z_{ref}(0) = 1\,\text{m}$, while external disturbances are neglected to isolate the effect of the chattering-reduction mechanism. The HGA algorithm is activated near the sliding manifold, where the discontinuous control term is replaced by a filtered counterpart using the low-pass transfer function $G_{NPF}(s) = \frac{K}{Ts+1}$. The HGA parameters are adopted from [3] without modification. The results clearly illustrate the expected trade-off: as shown in Fig. 2 and Fig. 3 (a), the original NTSMC achieves slightly better tracking performance, while NTSMC-HGA introduces modest transient deviations and slower convergence to the sliding manifold. In contrast, the control inputs in Fig. 3 (b) show a significant reduction of high-frequency switching under HGA, with considerably smoother signals after the transient phase, indicating effective chattering attenuation. Therefore, although HGA reduces chattering, this improvement comes at the expense of tracking accuracy and robustness. Consequently, the original

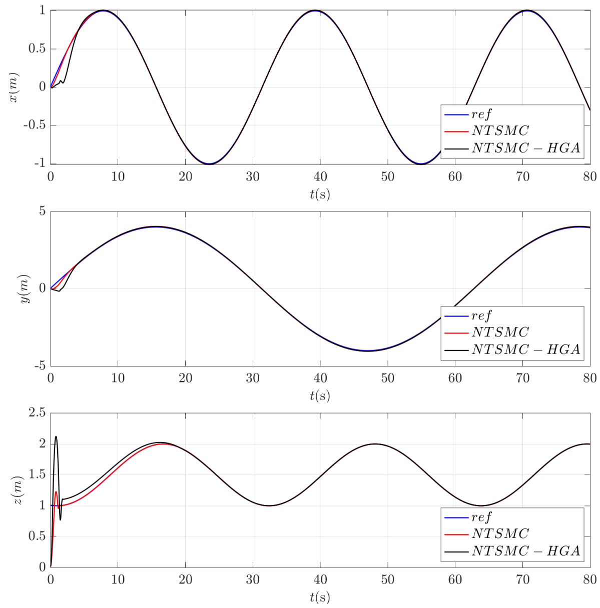

Fig. 2: Time responses of the quadrotor UAV position (Scenario 1)

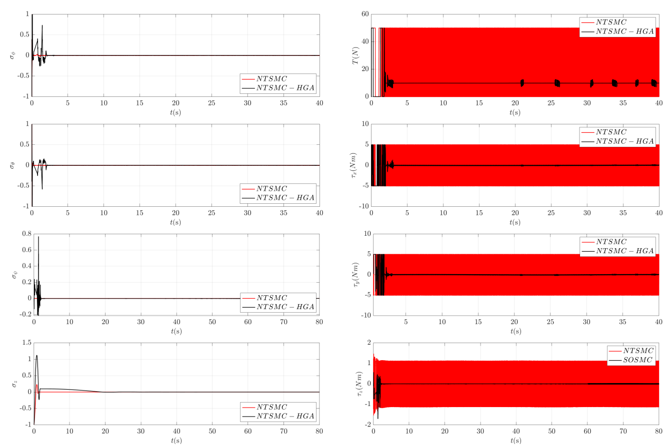

(a) Sliding variables (b) Control inputs

Fig. 3: Trade-off between control performance and chattering attenuation using HGA mechanism (Scenario 1)

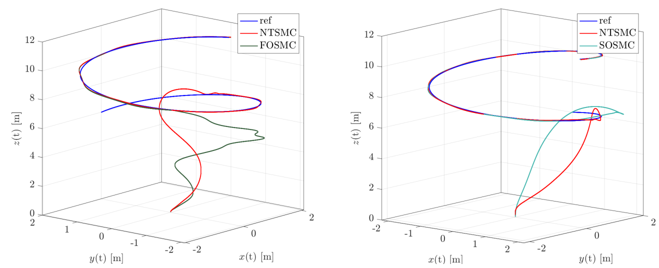

(a) (b)

Fig. 4: 3D trajectory tracking using the FOSMC, SOSMC and NTSMC under matched and unmatched non-vanishing disturbances (Scenario 2)

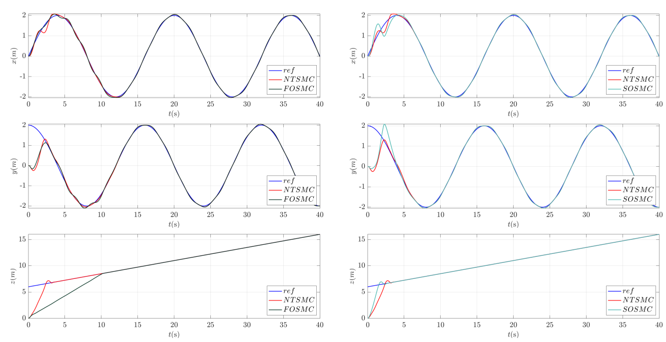

(a) (b)

Fig. 5: Position of the quadrotor UAV using the FOSMC, SOSMC and NTSMC under matched and unmatched non-vanishing disturbances (Scenario 2)

NTSMC controller is retained in subsequent scenarios, where robustness under disturbances is of primary interest.

Scenario 2 - Robustness properties and tracking performance under non-vanishing disturbances

In this scenario, the FOSMC, SOSMC, and NTSMC controllers are evaluated under identical perturbed initial conditions, with $y_{ref}(0) = 2$ and $z_{ref}(0) = 6$, and in the presence of three non-vanishing matched disturbances d_{τ_x}, d_{τ_y}, and d_{τ_z}, as well as two non-vanishing unmatched disturbances defined as $d_\phi(t) = d_\theta(t) = \sin(3t)$ acting through channels (16) and (17). The objective is to assess the robustness of the controllers under simultaneous perturbations and external disturbances. As shown in Fig. 4 and Fig. 5, the comparison between the controllers highlights different dynamic characteristics. FOSMC provides smoother lateral tracking during the transient phase, while NTSMC achieves faster and more stable altitude convergence (see Fig. 4 (a) and Fig. 5 (a)). In comparison with SOSMC, both controllers maintain convergence; however, NTSMC demonstrates smaller oscillations in the lateral motion, while SOSMC improves altitude tracking accuracy durung the transient (see Fig. 4 (b) and Fig. 5 (b)).

The results obtained in this scenario indicate that the SOSMC and the proposed NTSMC provide the most balanced performance in terms of convergence speed, tracking accuracy, and disturbance rejection. However, in order to further evaluate the robustness of the control strategies under more demanding operating conditions, an additional scenario involving aggressive maneuvers and persistent disturbances is considered in the following subsection.

Scenario 3 – Robustness under aggressive maneuvers and persistent disturbances

In the final scenario, the comparison is continued between NTSMC and SOSMC only, since SOSMC demonstrated stronger performance than FOSMC in the previous study and therefore represents a more demanding benchmark. The system is subjected to persistent matched disturbances acting on τ_x, τ_y, and τ_z, together with unmatched disturbances acting through ϕ and θ, all defined as $d(t) = \sin(3t)$. The scenario was selected to make tracking in the x-y plane more difficult and can therefore be viewed as a representative case of lateral wind-like disturbance. The results presented in Fig. 6

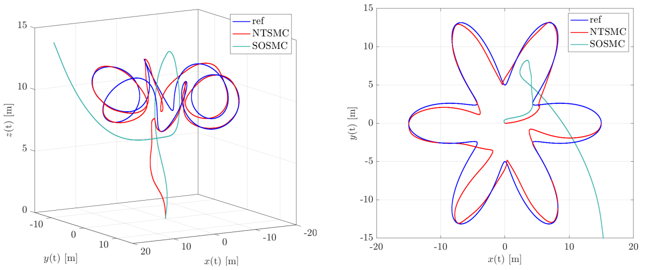

Fig. 6: Quadrotor UAV tracking of 3D trajectory with (x, y) planar projection using NTSMC and SOSMC under matched and unmatched non-vanishing disturbances and aggressive maneuvers (Scenario 3)

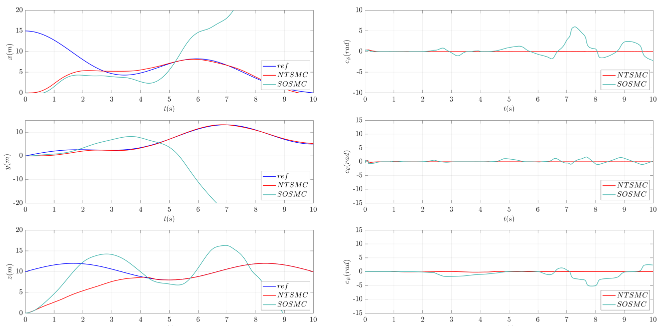

Fig. 7: Position coordinates and orientation tracking errors of the quadrotor UAV using NTSMC and SOSMC under matched and unmatched non-vanishing disturbances and aggressive maneuvers (Scenario 3)

and Fig. 7 show a clear difference between the controllers. While SOSMC gradually loses convergence and deviates from the desired trajectory, NTSMC maintains bounded and stable tracking throughout the simulation. Although SOSMC reaches the desired altitude slightly faster, this response is accompanied by significant overshoot, indicating aggressive control action. Consequently, the proposed NTSMC controller demonstrates superior robustness and more reliable trajectory tracking under aggressive operating conditions and strong disturbances.

V. CONCLUSIONS

This paper has presented an NTSMC strategy for robust 3D trajectory tracking of a quadrotor UAV in the presence of matched and unmatched disturbances. The main contribution of this work lies in the development and evaluation of an NTSMC-based control framework that achieves a favorable trade-off between robustness, convergence speed, and tracking accuracy under disturbed conditions. Stability analysis confirms finite-time convergence of the sliding variables and tracking errors under bounded disturbances, while simulation results validate the proposed approach under increasingly demanding scenarios. In particular, the proposed controller demonstrates improved altitude control and more balanced overall performance compared to FOSMC and SOSMC approaches. In addition, the HGA mechanism has been incorporated to mitigate chattering effects inherent to discontinuous control laws. The obtained results highlight the trade-off between chattering reduction and robustness, showing that improved control smoothness is achieved at the expense of reduced disturbance rejection capability.

REFERENCES

[1] M. Blösch, S. Weiss, D. Scaramuzza, and R. Siegwart, "Vision based mav navigation in unknown and unstructured environments," in *2010 IEEE International Conference on Robotics and Automation*, 2010, pp. 21–28.

[2] A. Salihbegovic, V. Capin, E. Sokic, and N. Osmic, "Trajectory tracking of the octo-rotor unmanned aerial vehicle exposed to parametric uncertainties and external disturbances using first order sliding mode control," in *2023 XXIX International Conference on Information, Communication and Automation Technologies (ICAT)*, 2023, pp. 1–8.

[3] F. Tahirovic, A. Salihbegovic, E. Sokic, and N. Osmic, "Enhanced robustness properties and tracking performance of the quadrotor unmanned aerial vehicle under disturbances via the second order sliding mode control," in *2024 10th International Conference on Control, Decision and Information Technologies (CoDIT)*, 2024, pp. 1141–1146.

[4] F. Tahirovic, A. Salihbegovic, E. Sokic, N. Osmic, and S. Konjicija, "Twisting sliding mode control of a nonlinear quadrotor uav under perturbations and disturbances," in *2024 International Symposium ELMAR*, 2024, pp. 307–310.

[5] S. Bouabdallah, A. Noth, and R. Siegwart, "Pid vs lq control techniques applied to an indoor micro quadrotor," in *2004 IEEE/RSJ International Conference on Intelligent Robots and Systems (IROS)(IEEE Cat. No. 04CH37566)*, vol. 3. IEEE, 2004, pp. 2451–2456.

[6] S. Bouabdallah and R. Siegwart, "Backstepping and sliding-mode techniques applied to an indoor micro quadrotor," in *Proceedings of the 2005 IEEE international conference on robotics and automation*. IEEE, 2005, pp. 2247–2252.

[7] A. Salihbegovic, A. Talic, N. Osmic, and E. Sokic, "3d trajectory tracking of a quad-rotor unmanned aerial vehicle via the first order sliding mode control," in *2023 9th International Conference on Control, Decision and Information Technologies (CoDIT)*, 2023, pp. 1530–1535.

[8] R. Xu and U. Ozguner, "Sliding mode control of a quadrotor helicopter," in *Proceedings of the 45th IEEE Conference on Decision and Control*, 2006, pp. 4957–4962.

[9] R. Xu and Ümit Özgüner, "Sliding mode control of a class of underactuated systems," *Automatica*, vol. 44, no. 1, pp. 233–241, 2008.

[10] H. Wang, X. Ye, Y. Tian, G. Zheng, and N. Christov, "Model-free–based terminal smc of quadrotor attitude and position," *IEEE Transactions on Aerospace and Electronic Systems*, vol. 52, no. 5, pp. 2519–2528, 2016.

[11] F. Chen, R. Jiang, K. Zhang, B. Jiang, and G. Tao, "Robust backstepping sliding-mode control and observer-based fault estimation for a quadrotor uav," *IEEE Transactions on Industrial Electronics*, vol. 63, no. 8, pp. 5044–5056, 2016.

[12] A. Salihbegovic, "Multivariable sliding mode approach with enhanced robustness properties based on the robust internal-loop compensator for a class of nonlinear mechanical systems," in *2016 European Control Conference (ECC)*, 2016, pp. 382–387.

[13] ——, "Robust internal-loop compensator based sliding mode control of nonlinear systems in the presence of mismatched disturbances," *IEEE Access*, vol. 7, pp. 50 492–50 502, 2019.

[14] B. Mu, K. Zhang, and Y. Shi, "Integral sliding mode flight controller design for a quadrotor and the application in a heterogeneous multi-agent system," *IEEE Transactions on Industrial Electronics*, vol. 64, no. 12, pp. 9389–9398, 2017.

[15] H. Ríos, R. Falcón, O. A. González, and A. Dzul, "Continuous sliding-mode control strategies for quadrotor robust tracking: Real-time application," *IEEE Transactions on Industrial Electronics*, vol. 66, no. 2, pp. 1264–1272, 2019.

[16] O. Mofid and S. Mobayen, "Robust fractional-order sliding mode tracker for quad-rotor uavs: Event-triggered adaptive backstepping approach under disturbance and uncertainty," *Aerospace Science and Technology*, vol. 146, p. 108916, 2024.

[17] C. Rosales, C. V. Sisterna, F. Rossomando, D. Gandolfo, C. Soria, and R. Carelli, "Super-twisting adaptive control of a quadrotor," *ISA Transactions*, 2025.

[18] N. Osmic, A. Tahirovic, and B. Lacevic, "Octocopter design: Modelling, control and motion planning," *arXiv:2212.01210*, 2022.